Bulk photovoltaic effect in a zero-dimensional room-temperature molecular ferroelectric $[C_8N_2H_{22}]_{1.5}[Bi_2I_9]$

Zhibo Chen,[a] Tianhong Luo,[a] Jinrong Wen,[a] Zhanqiang Liu,[b] Jingshan Hou,[a] Yongzheng Fang*,[a] and Ganghua Zhang*,[a]

[a]*School of Materials Science and Engineering, Shanghai Institute of Technology, Shanghai 201418, P. R. China;*

[b]*Department of Materials Chemistry, Huzhou University, 759 East Erhuan Road, Huzhou, 313000, P. R. China.*

E-mail addresses: ganghuazhang@sit.edu.cn (G.H. Zhang) and fyz1003@sina.com (Y.Z. Fang)

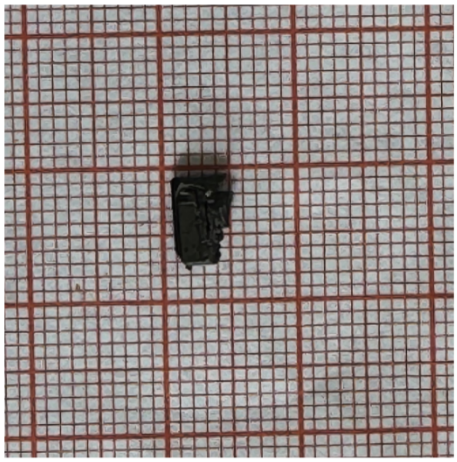

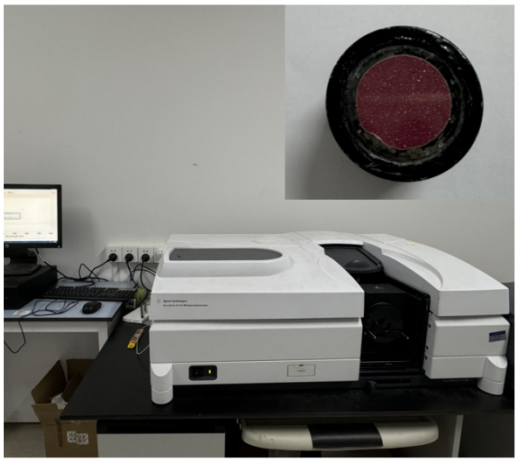

Fig. S1 Bulk crystal for hysteresis loop tests (a) and the photograph for the UV-Vis measurement (b).

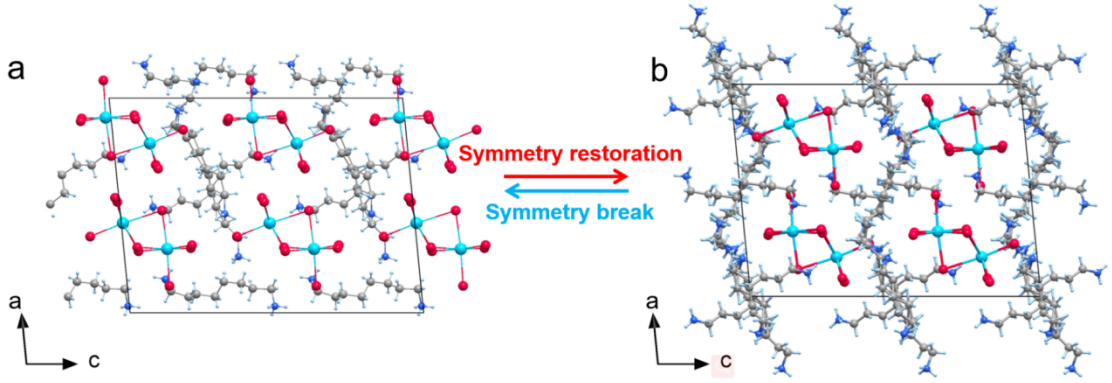

Fig. S2 Schematic diagram of ferroelectric to paraelectric phase transition in $[C_8N_2H_{22}]_{1.5}[Bi_2I_9]$.

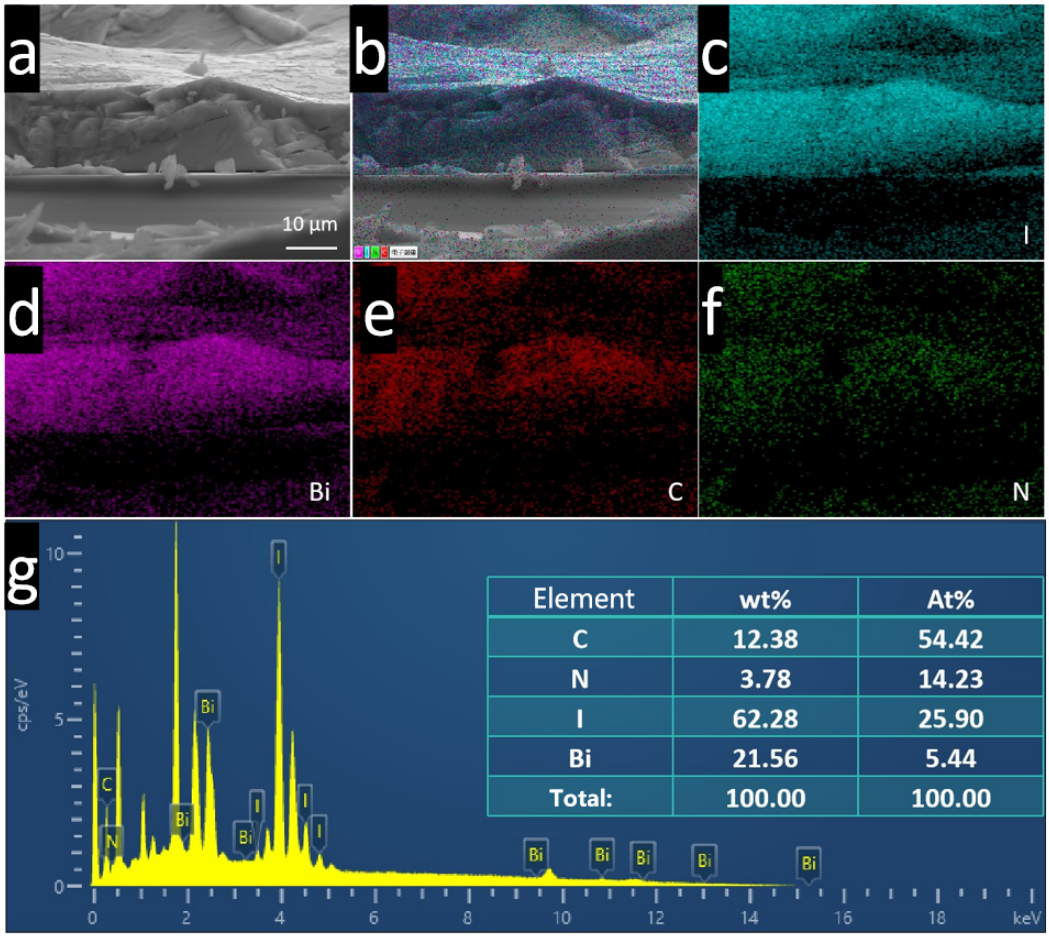

Fig. S3 Mapping images (a-f) and EDS results (g) of $[C_8N_2H_{22}]_{1.5}[Bi_2I_9]$ film.

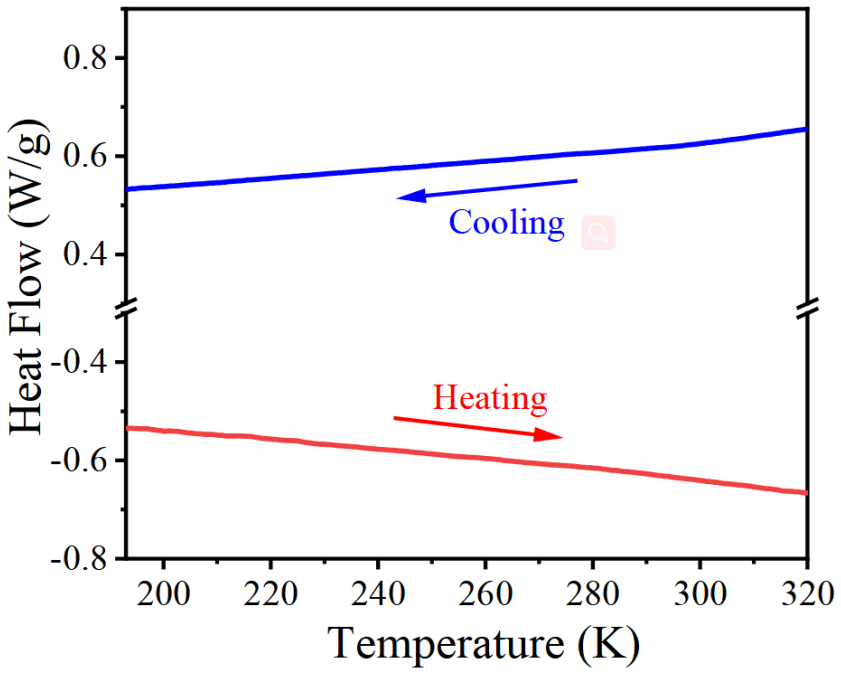

Fig. S4 Low-temperature DSC curve of $[C_8N_2H_{22}]_{1.5}[Bi_2I_9]$.

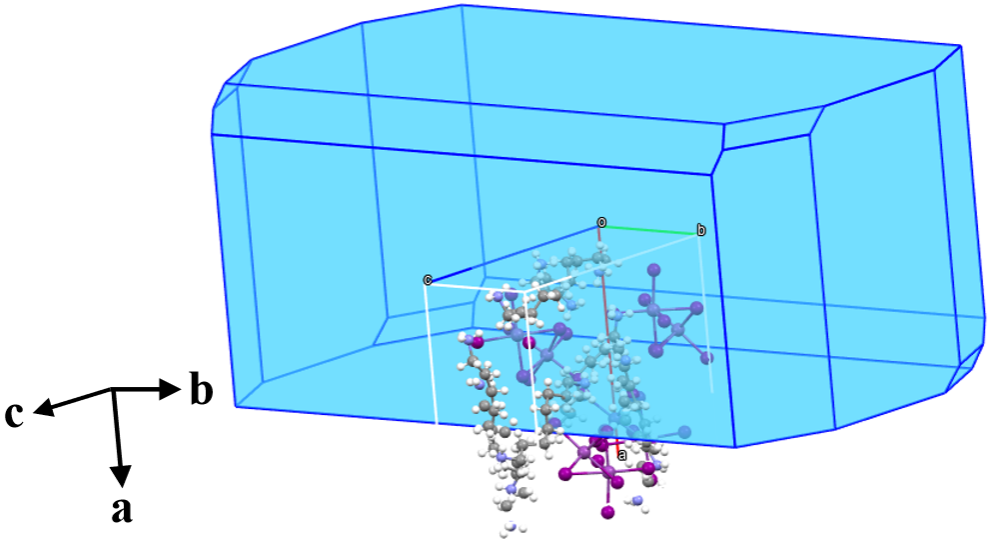

Fig. S5 Crystal morphology of $[C_8N_2H_{22}]_{1.5}[Bi_2I_9]$ with polarization labeling.

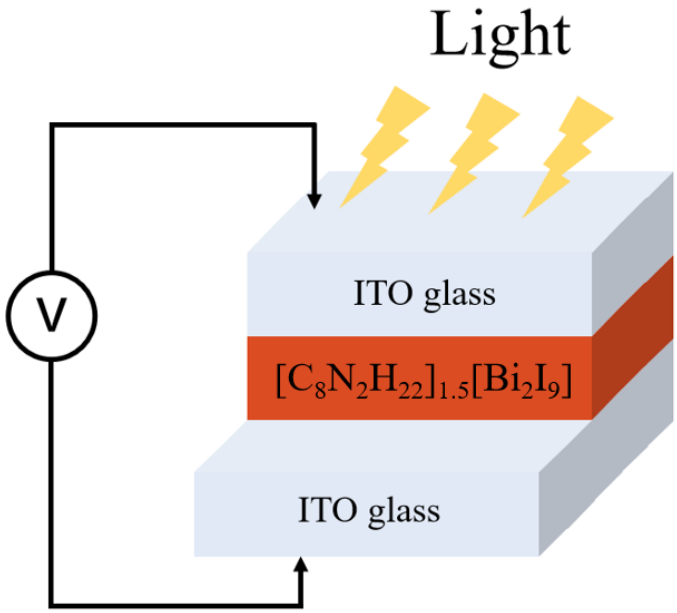

Fig. S6 Schematically setup of $[C_8N_2H_{22}]_{1.5}[Bi_2I_9]$-based photoelectric device.

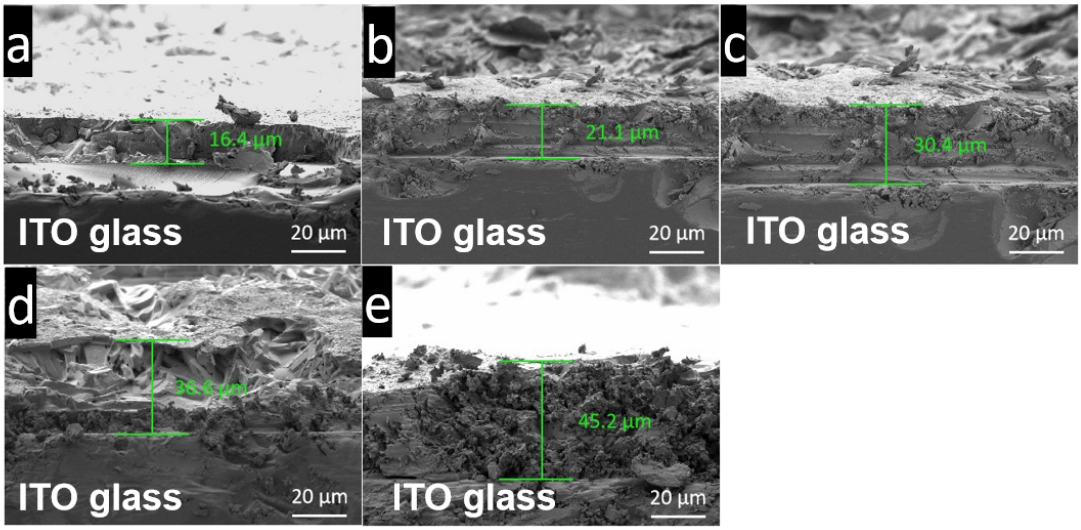

Fig. S7 Cross-sectional SEM images of $[C_8N_2H_{22}]_{1.5}[Bi_2I_9]$/ITO thin films with different thicknesses.

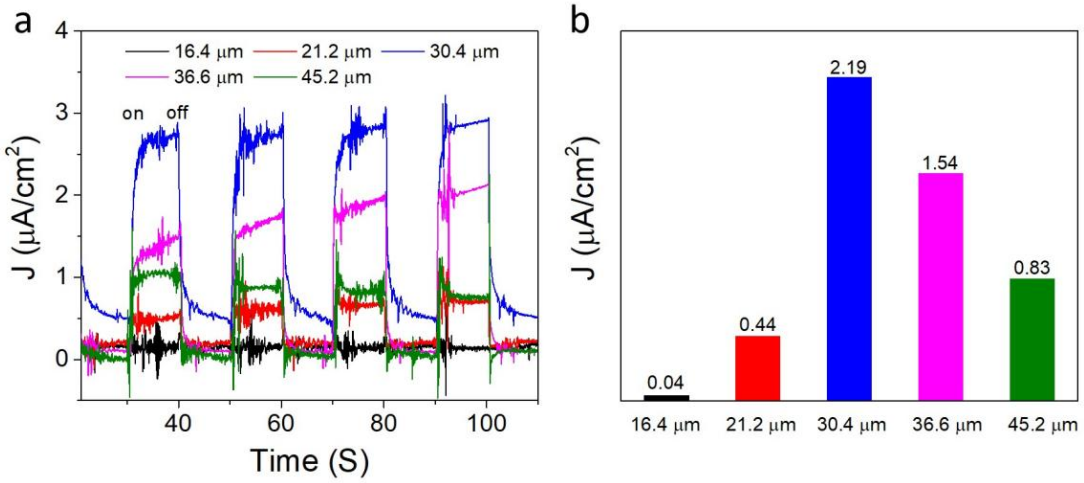

Fig. S8 (a) Zero-voltage *J-t* curves of $[C_8N_2H_{22}]_{1.5}[Bi_2I_9]$-based photoelectric devices with different thicknesses. (b) Thickness-dependent photocurrent densities of $[C_8N_2H_{22}]_{1.5}[Bi_2I_9]$-based photoelectric devices

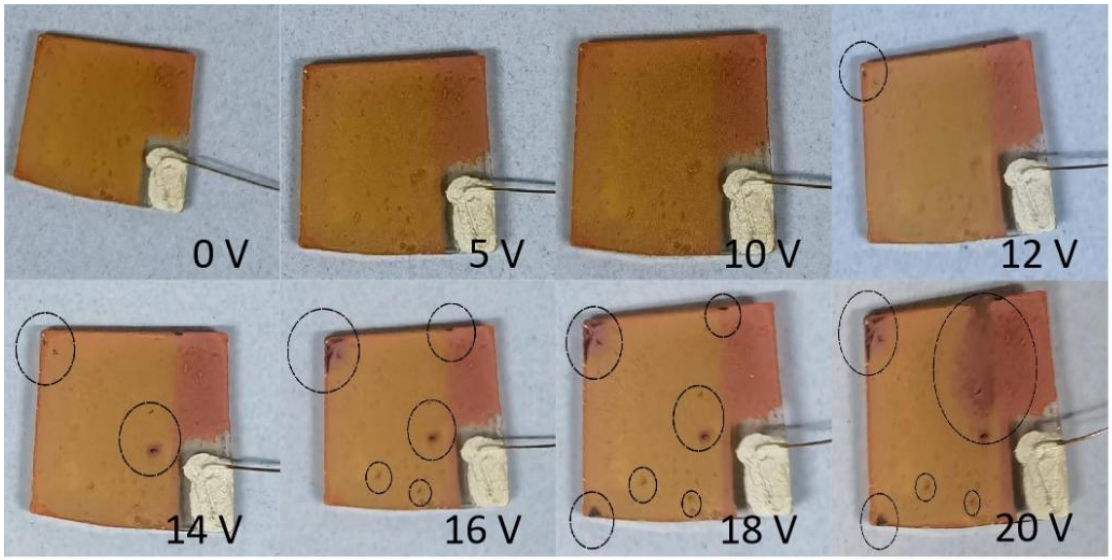

Fig. S9 Physical appearance of $[C_8N_2H_{22}]_{1.5}[Bi_2I_9]$-based photoelectric device under different polarization voltages (dashed circles indicate breakdown regions under high polarization voltages).

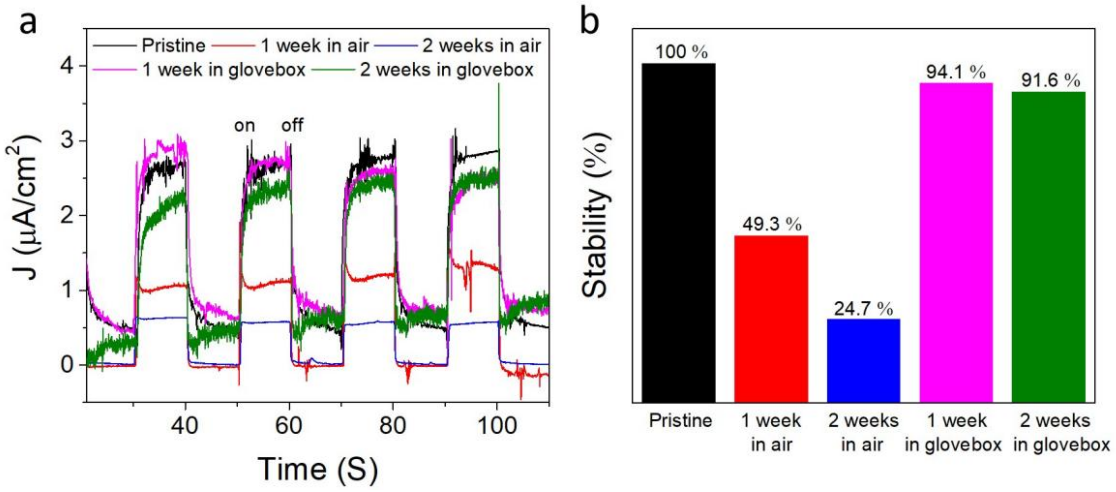

Fig. S10 (a) Zero-voltage *J-t* curves of $[C_8N_2H_{22}]_{1.5}[Bi_2I_9]$-based photoelectric device after exposing to the atmosphere and glovebox conditions for different time. (b) Corresponding photocurrent degeneration rate over time.

Table S1. Atomic coordinates for Bi, N and I in $[C_8N_2H_{22}]_{1.5}[Bi_2I_9]$.

Elements（charge）	Numbers	coordinate
Bi^{3+}	8	（0.5826, 0.5028, 0.5244）
N^{+}	16	（0.3705, 0.5027, 0.4749）
I^{-}	36	（0.5422, 0.4988, 0.4780）

Point charge model analyses

According to the crystallographic data of $[C_8N_2H_{22}]_{1.5}[Bi_2I_9]$, we select a unit cell and assume that the centers of the positive charges of the cations are located on the N atoms and Bi atoms, the negative charges of the anions are located on the I atoms.

Along *a*-axis

$$P_s = \lim \frac{1}{V} \Sigma q_i r_i$$

$$= (q_N r_N + q_{Pb} r_{Pb} - q_I r_I) / V$$

$$= \left| (0.5826 \times 8 \times 3 + 0.3705 \times 16 - 0.5422 \times 36) \right| \times 1.6 \times 10^{-19} \times 17.5341 \times 10^{-10} / 3557.5 \times 10^{-30}$$

$$= 0.00308 \text{ C/cm}^2$$

$$\left| P_s \right| = 3.08 \ \mu\text{C/cm}^2$$

Along *c*-axis

$$P_s = \lim \frac{1}{V} \Sigma q_i r_i$$

$$= (q_N r_N + q_{Pb} r_{Pb} - q_I r_I) / V$$

$$= \left| (0.5244 \times 8 \times 3 + 0.4749 \times 16 - 0.4780 \times 36) \right| \times 1.6 \times 10^{-19} \times 23.945 \times 10^{-10} / 3557.5 \times 10^{-30}$$

$$= 0.0032 \text{ C/cm}^2$$

$$\left| P_s \right| = 3.2 \ \mu\text{C/cm}^2$$

Table S2. Crystallographic data and refinement parameters of $[C_8N_2H_{22}]_{1.5}[Bi_2I_9]$ single crystal at 193 K conditions.

Empirical formula	$[C_8N_2H_{22}]_{1.5}[Bi_2I_9]$
Formula weight	1779.47
Temperature/K	193.0
Crystal system	monoclinic
Space group	*Pc*
a/Å	17.5314(16)
b/Å	8.5135(8)
c/Å	23.945(2)
α/°	90
β/°	95.581(3)
γ/°	90
Volume/Å^3	3557.5(6)
Z	2
ρ_{calc}g/cm^3	3.322
μ/mm^{-1}	17.696
F(000)	3076.0
Crystal size/mm^3	0.12 × 0.08 × 0.01
Radiation	MoKα (λ = 0.71073)
2θ range for data collection/°	3.948 to 52.744
Index ranges	$-21 \le h \le 21$, $-10 \le k \le 9$, $-29 \le l \le 29$
Reflections collected	25936
Independent reflections	13527 [R_{int} = 0.0485, R_{sigma} = 0.0670]
Data/restraints/parameters	13527/665/566
Goodness-of-fit on F^2	1.019
Final R indexes [I>=2σ (I)]	R_1 = 0.0468, wR_2 = 0.1139
Final R indexes [all data]	R_1 = 0.0678, wR_2 = 0.1299
Largest diff. peak/hole / e Å^{-3}	1.77/-1.61